

# Microstructural and In-Vitro Characterization of Glass-Reinforced Hydroxyapatite Composites

Uma Batra and Seema Kapoor

**Abstract**—Commercial hydroxyapatite (HA) was reinforced by adding 2, 5, and 10 wt % of 28.5%CaO-28.5%P<sub>2</sub>O<sub>5</sub>-38%Na<sub>2</sub>O-5%CaF<sub>2</sub> based glass and then sintered. Although HA shows good biocompatibility with the human body, its applications are limited to non load-bearing areas and coatings due to its poor mechanical properties. These mechanical properties can be improved substantially with addition of glass ceramics by sintering. In this study, the effects of sintering hydroxyapatite with above specified phosphate glass additions are quantified. Each composition was sintered over a range of temperatures. Scanning electron microscopy and x-ray diffraction were used to characterize the microstructure and phases of the composites. The density, microhardness, and compressive strength were measured using Archimedes Principle, Vickers Microhardness Tester (at 0.98 N), and Instron Universal Testing Machine (cross speed of 0.5 mm/min) respectively. These results were used to indicate which composition provided suitable material for use in hard tissue replacement. Composites containing 10 wt % glass additions formed dense HA/TCP (tricalcium phosphate) composite materials possessing good compressive strength and hardness than HA. In-vitro bioactivity was assessed by evaluating changes in pH and Ca<sup>2+</sup> ion concentration of SBF-simulated body fluid on immersion of these composites in it for two weeks.

**Keywords**—Bioglass, Composite, Hydroxyapatite, Sintering.

## I. INTRODUCTION

**H**YDROXYAPATITE (HA), at present, is of great interest as a material for surgical implants, due to its biocompatibility with living tissue. Connective tissue, which holds together the different structures in the body, is inherent in bone and contains collagen fibres, mineral part and ground substance. The exact composition and relative proportions of collagen depend upon numerous factors, including the location and loading requirements of bone [1-3]. Structural and chemical analyses of the inorganic part of bone have shown that ionic substitutions may occur within the HA lattice [2]. Substitutions include CO<sub>3</sub><sup>2-</sup> for OH<sup>-</sup> or PO<sub>4</sub><sup>3-</sup>, Mg<sup>2+</sup> and Na<sup>+</sup> for Ca<sup>2+</sup>, and F<sup>-</sup> for PO<sub>4</sub><sup>3-</sup> [2]. Such substitutions lead to the change in the lattice parameters and in turn affect the stability of HA as well as tricalcium phosphate (TCP) phase [4]. Thus, it is important to incorporate these trace elements in orthopedic implants, such as HA, because the biocompatibility of apatites is closely dependent on their composition [5]. The main reason for developing and

producing composite materials is to achieve a combination of properties not achievable by any of the elemental materials alone. The glasses within P<sub>2</sub>O<sub>5</sub>-CaO system are considered to have enormous potential as biomaterials. Synthetic HA is limited in its use as a biomaterial, primarily due to its low load bearing capacity which can be illustrated by the relatively poor mechanical properties compared with bone [6-11]. However, improvements on its mechanical properties have been undertaken with the inclusion of soluble phosphate based glasses (P<sub>2</sub>O<sub>5</sub>-CaO-Na<sub>2</sub>O) [6-11]. Phosphate glasses, when incorporated into HA, melt at a lower temperature compared to HA and can act to increase density by enhancing the sintering mechanisms which greatly enhances the mechanical properties. Furthermore, decomposition of HA into secondary phases,  $\alpha$ - and  $\beta$ -TCP, can occur.

Tricalcium phosphate (TCP) a crystalline bioactive ceramic also degrades to calcium and phosphate salts both in-vivo and in-vitro, and also results in the precipitation of hydroxyapatite on the surface of an implant [12]. Several studies with  $\beta$ -TCP and biphasic HA/ $\beta$ -TCP ceramics have shown that  $\beta$ -TCP behaves in an osteoinductive manner enhancing bone in-growth around and into implants in animal studies [13, 14]. In a separate study using a mixture of hydroxyapatite with TCP with autogenous cancellous bone, it was shown that there was strong callus formation and a strong bony union after four weeks of implantation [15]. Among all the calcium phosphates used in biological applications only two calcium phosphates are stable when they are in contact with aqueous media: At a pH<4.2 the stable phase is CaHPO<sub>4</sub>·2H<sub>2</sub>O (DCP) while at pH>4.3 the stable phase is hydroxyapatite [16]. Furthermore, different calcium phosphates have different induction time for the formation of carbonated apatite with some of the calcium deficient hydroxyapatite exhibiting poor bioactivity while the TCP and calcium pyro phosphates exhibiting very good bioactivity [16]. There have been many attempts to combine hydroxyapatite with bioactive glasses of different compositions in order to produce composites with improved mechanical and biological properties [17-19] and significant gains in mechanical properties with improved bioactivity have been reported.

The effects of phosphate glass additions, from the system P<sub>2</sub>O<sub>5</sub>-CaO-Na<sub>2</sub>O-CaF<sub>2</sub>, on the sintering, phase composition, and mechanical properties of HA are analysed in this study. The main aim is to provide a comprehensive insight about the mechanical properties and possible biocompatibility of such composites, which should help to determine the optimum composites for use as implant materials.

Dr. Uma Batra is with the Deptt. of Metallurgical Engineering, PEC University of Technology, Chandigarh-160012, India (corresponding author; phone: +91-9501013054; fax: +91-172-2745175; e-mail: umabatra2@yahoo.com).

Dr. Seema Kapoor is with the Univ. Institute of Chemical Engineering & Technology, Panjab University, Chandigarh-160014, India. (e-mail: seemakap\_2004@sify.com).

## II. MATERIALS AND METHODS

### A. Specimen Preparation

Phosphate based glass containing 28.5, 28.5, 38, and 5 wt % of CaO, P<sub>2</sub>O<sub>5</sub>, Na<sub>2</sub>O, and CaF<sub>2</sub> were prepared by mixing 8.55 gm of CaCO<sub>3</sub>, 1.5 gm of CaF<sub>2</sub> with 11.4 gm of Na<sub>2</sub>CO<sub>3</sub> (Merck Ltd.) to which orthophosphoric acid (H<sub>3</sub>PO<sub>4</sub>) was added gradually. During this the mixture was continuously mixed using mortar and pestle. 5 ml of H<sub>3</sub>PO<sub>4</sub> acid was added in total. The mixture was preheated in oven for 30 minutes followed by transferring it to the muffle furnace maintained at 900°C for 4 hours till solid crystalline mass appeared.

HA powder was then mixed with various proportion of 2 wt %, 5 wt %, and 10 wt % of bioglass to form three HA based reinforced ceramics denoted as HA-B1, HA-B2, and HA-B3 respectively. The said mixture was prepared by mixing the contents for about 5 hours in a mortar and pestle.

All the above compositions were compacted to prepare the green pellets. For this 1gm of each composition was uniaxial compacted in a cylindrical die of 15 mm diameter using a compaction load of 20 kgf resulting in disc pellets.

The green pellets prepared were subjected to sintering in a micro-controller temperature furnace. The samples were heated at a rate of 2°C/min, soaked at 100°C for 10 minutes, followed by further heating to 550°C, where it was soaked for 30 minutes to allow annealing of samples. The temperature was further raised to 1250°C using the same heating rate of 2°C/min. After soaking for 3 hours, the samples were cooled gradually to 850°C in 3 hours, where these were soaked for 30 minutes, followed by their cooling to room temperature in 2 hours.

### B. Density Determination

Density measurements were performed on each sintered specimen using the Archimedes principle. 8 to 10 samples were used to determine the average density for each group.

### C. Mechanical Testing

Vickers hardness was measured using a Vickers Microhardness Tester (at 0.98 N) and compression test was performed using Instron Universal Testing Machine (cross speed of 0.5 mm/min) respectively.

### D. X-Ray Diffraction

Phase analysis for sintered bioglass, hydroxyapatite, and hydroxyapatite-bioglass composites was performed by X-Ray diffraction using a Philips Xpert diffractometer with CuK $\alpha$  (1.54Å) radiation. The data were recorded over the 2 $\theta$  range of 20° to 70° with a 0.017° step size and scan step time of 20.03 s. The phases present in HA, bioglass, HA reinforced ceramics HA-B1, HA-B2, and HA-B3, were identified using JCPDS file 03-0407. In compositions HA, HA-B1, HA-B2, and HA-B3, the peaks for HA were identified for Ca<sub>10</sub>(PO<sub>4</sub>)<sub>6</sub>OH<sub>2</sub>.

The peak broadening of XRD pattern was used to estimate the crystallite size in a direction perpendicular to the crystallographic plane based on Scherrer's formula as follows (1):

$$X_s = 0.9\lambda / FWHM \cos \theta \quad (1)$$

where X<sub>s</sub> is the crystallite size in nm,  $\lambda$  the wave length of X-ray beam ( $\lambda = 0.15406$ nm for CuK $\alpha$  radiation), FWHM the full

width at half maximum for the diffraction peak under consideration (rad), and  $\theta$  is the diffraction angle (°). The diffraction peak at  $2\theta = 25.99^\circ$  was chosen for calculation of crystallite size since it was sharper and isolated from others. This peak assigns to (002) Miller's plane family and shows the crystal growth along the c-axis of the hydroxyapatite crystalline structure.

The fraction of crystalline phase (X<sub>c</sub>) was evaluated as follows (2):

$$X_c = 1 - V_{112/300} / I_{300} \quad (2)$$

where I<sub>300</sub> is the intensity of (300) diffraction peak and V<sub>112/300</sub> is the intensity of the hollow between (112) and (300) diffraction peaks of hydroxyapatite.

The lattice parameters for HA, HA-B1, HA-B2, and HA-B3 are given in Table I.

### Scanning Electron Microscopy (SEM)

Microstructures for all sintered materials were examined using a SEM JSM 6100. All these sintered samples were made conducting by sputter coating with gold in a sputtering machine JFC 1100. The micrographs were used to study the nature of bonding, distribution of bioglass particles, and the morphology of the phases in HA, HA-B1, HA-B2, and HA-B3 compositions.

TABLE I  
LATTICE PARAMETERS FOR HA/PHOSPHATE GLASS COMPOSITES

Composition	a (Å)	c (Å)	Crystallite size(nm)	Crystallinity (%)
HA	9.886	6.8540	71.7	79.0
HA-B1	9.949	6.9209	70.4	81.7
HA-B2	9.836	6.8660	69.3	77.0
HA-B3	9.908	6.8460	59.2	74.0

### Bioactivity (In Vitro) Characterisation

The dissolution behaviour of HA and the composites was performed by their immersion for 2 weeks in a simulated body fluid (SBF) medium of pH 7.4 at a ratio of 1mg/ml in a water bath at 37°C. The SBF medium consisted of 9g NaCl, 5g KCl and 0.2g MgHPO<sub>4</sub>.3H<sub>2</sub>O per litre. The changes in pH were measured at pre-determined time intervals using pH meter. The dissolution of calcium ions in SBF medium was determined by an atomic absorption spectrometer (AAS).

## III. RESULTS AND DISCUSSION

Figs. 1-3 show the variation in density, microhardness, and compressive strength with change in reinforcement content. Fig. 1 indicates that HA-glass composites have higher density values compared to HA and the density increases with the increase in the bioglass addition from 2 wt % to 10 wt %. Also, from Fig. 2, it can be seen that the hardness increases with the increase in reinforcement content.

Compression test results of HA/bioglass composites showed substantially higher strength values compared to HA sintered bodies. While strength has been observed 41±20 MPa for HA, it obtained interesting values for HA-B1, HA-B2, and HA-B3 compositions as can be seen from Fig. 3. It can be observed

that increasing reinforcement content increases compressive strength. The reason for high standard deviation values can be attributed to brittleness character of HA.

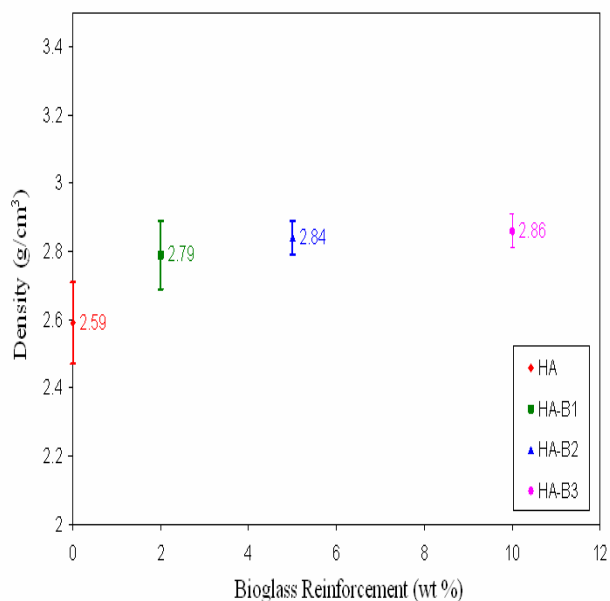


Fig.1. Variation in density with bioglass reinforcement content

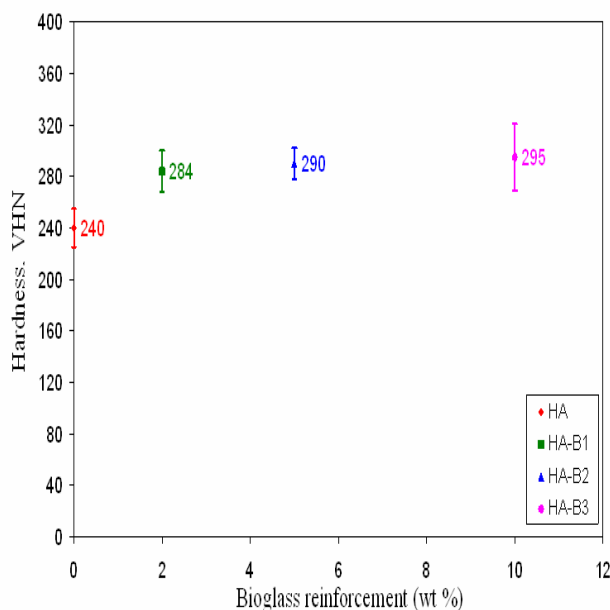


Fig. 2. Variation in hardness with bioglass reinforcement content

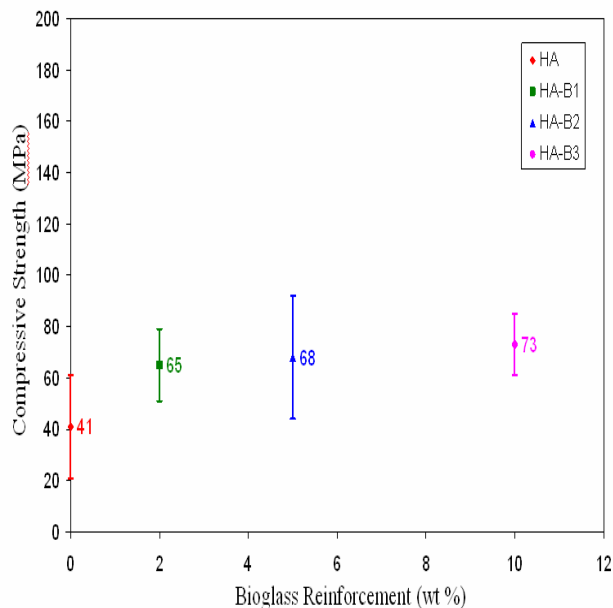


Fig.3. Variation in compressive strength with bioglass reinforcement content

Fig. 4 shows the XRD patterns of the four different HA reinforced ceramics and the analysis of the structure is listed in Table II. Identical pattern recorded for all these compositions suggest that the HA structure is retained even on addition of bioglass and sintering at 1250°C. The primary ceramic present when 2, 5, and 10 wt % bioglass was sintered with hydroxyapatite is hydroxyapatite with  $\beta$ -TCP ( $\text{Ca}_3(\text{PO}_4)_2$ ) as the secondary phase (JCPDF#03-0407). No other phases like  $\alpha$ -tricalcium phosphate ( $\alpha$ -TCP) and calcium oxide (CaO) were detected, which indicates that the bioglass behaves more as a sintering aid and promotes the conversion of HA to  $\beta$ -TCP.

It has already been reported by various researchers that same sintering aids promote formation of other phases like  $\alpha$ - and  $\beta$ -TCP, the amount and the rate of their formation depend on the sintering additive [20, 21]. The formation of small amounts of  $\beta$ -TCP is advantageous as it allows ionic substitutions and results in enhanced bioactivity.

The lattice parameters of HA and  $\beta$ -TCP changed as the percentage glass was increased, indicating a change in stoichiometry due to either lattice vacancies or substitutions.

TABLE II  
PHASES DEVELOPED DURING SINTERING OF HA WITH 2, 5, AND 10 WT % BIOGLASS

Bioglass (wt %)	Composition of Phases Present
0	Synthetic Hydroxyapatite ( $\text{Ca}_{10}(\text{PO}_4)_6\text{OH}_2$ )
2	Synthetic Hydroxyapatite + $\beta$ -TCP ( $\beta\text{-Ca}_3(\text{PO}_4)_2$ )
5	Synthetic Hydroxyapatite + $\beta$ -TCP
10	Synthetic Hydroxyapatite + $\beta$ -TCP

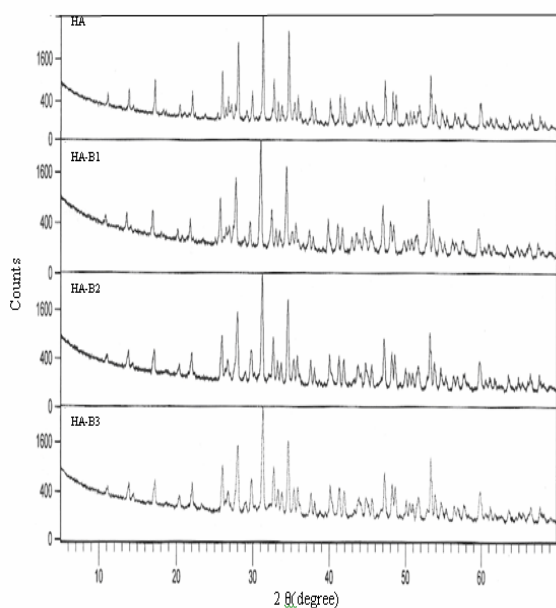


Fig. 4. Comparison of the XRD pattern for HA, HA-B1, HA-B2, and HA-B3

Fig. 5 shows SEM for 100 % HA, HA reinforced with 2 wt %, 5 wt %, and 10 wt % bioglass. SEM for 100% HA shows large agglomerates of HA crystals indicating very good bonding of the HA particles through solid phase sintering. The porosity is well distributed throughout the sample. Some liquid phase formation is also observed.

The Fig. 5(b) shows SEM for HA-B1 composition. It has been observed that particles have bonded mainly through the liquid phase sintering. Bioglass particles are found generally at or near to the grain boundary of HA. The porosity is smaller in size and more uniformly distributed.

SEM for HA-B2 composition (Fig.5(c)) shows quite similar features to those observed in micro-graph of HA-B1 composition. SEM micrograph shows the bonding of particles through the solid phase sintering as well as liquid phase sintering where as the liquid phase sintering appears more prominent as compared to solid phase sintering. Bioglass particles are found generally at or near to the grain boundary of HA. The porosity is smaller in size and more uniformly distributed.

Fig. 5(d) shows SEM for HA-B3 composition. Larger networks of HA have formed largely by the liquid phase sintering. The individual crystals or grains of HA are not clearly visible in the structure. This shows that the cooling after sintering at 1250°C for 3 hours did not allow the crystals to form.

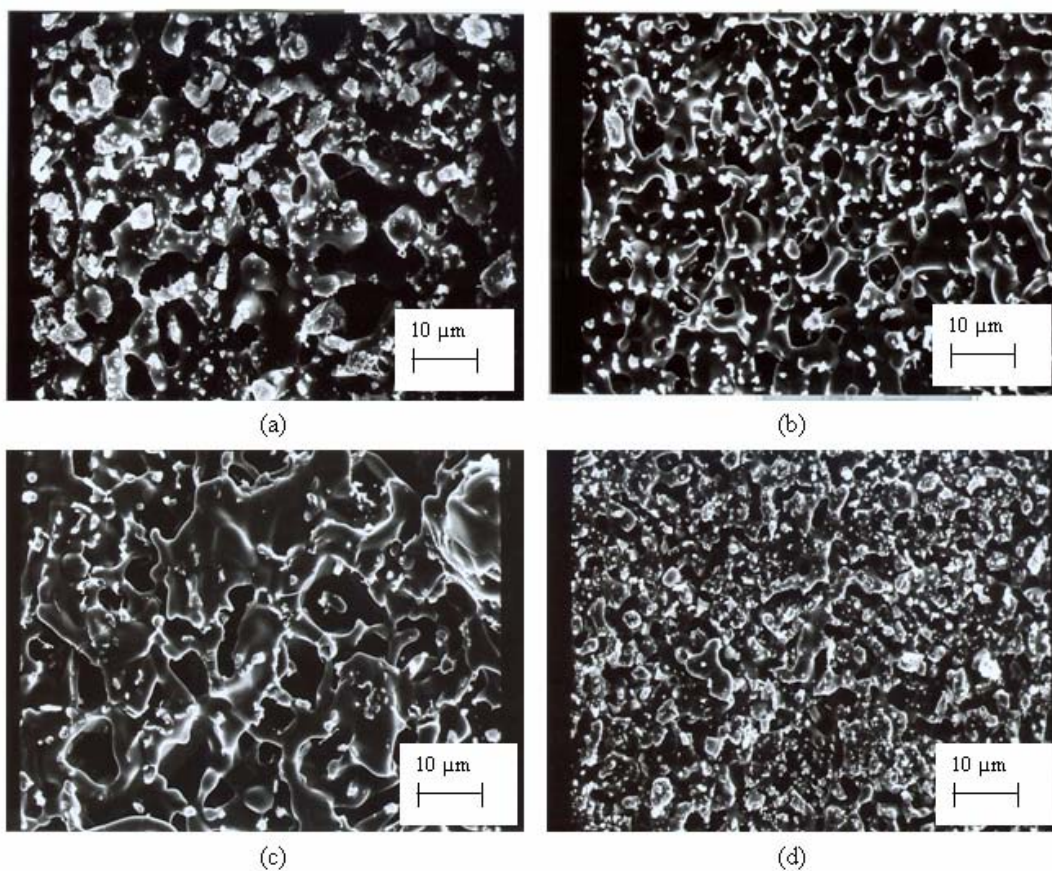


Fig. 5. SEM of (a) HA (b) HA-B1 composition (c) HA-B2 composition and (d) HA-B3 composition

As a result of the time, effort, cost, increasing restrictions, and lack of precise basic data derived from animal experimentation, in-vitro testing has become an important, major tool for evaluating the compatibility of new and modified materials for surgical application [22]. In order to determine the mineralization ability and bioactivity of each of these sintered bioceramics, the samples were immersed in SBF for 14 days. All surfaces exhibited dissolution coupled with mineralization. There are some important distinctions in the nature of dissolution and mineralization on the bioceramic surfaces as can be seen from Fig. 6 and Fig. 7. It has been observed that the pH of SBF medium is higher for 5 wt % and 10 wt % bioglass HA reinforced than 2 wt % reinforced HA with bioglass. The pure HA surface exhibited the least level of activity with the surface exhibiting some dissolution, on the other hand the composition with 2 wt % bioglass exhibited a fine layer of mineralization on the surface coupled with some dissolution. The composition with 5 wt % and 10 wt % bioglass exhibited larger levels of mineralization coupled with large dissolution of the glassy phase. The level of mineralization in these three chemistries increases with the amount of glassy phase.

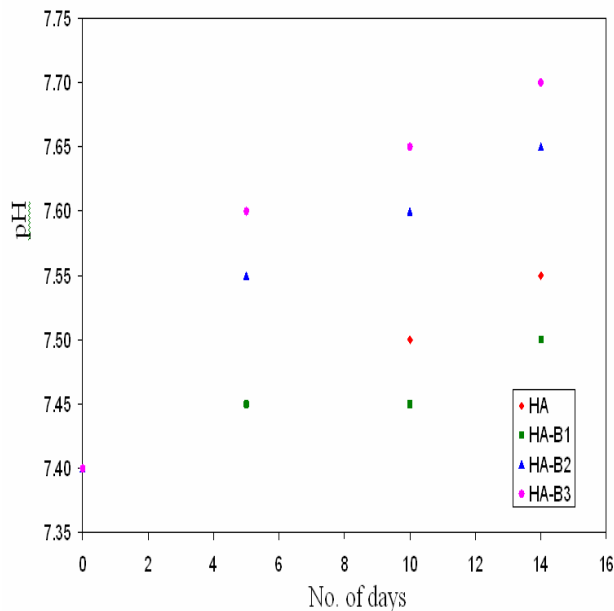


Fig.6. Change in pH of SBF medium with time

#### IV. CONCLUSION

The findings of this work are concluded as follows:-

- CaO-P<sub>2</sub>O<sub>5</sub>-Na<sub>2</sub>O-CaF<sub>2</sub> based glasses are closely related to the composition of hydroxyapatite.
- On sintering at 1250<sup>o</sup>C, the HA retains its structure in HA, with and without bioglass reinforcement. In addition to HA, small amount of β-TCP is observed in HA-Bioglass reinforced composites.

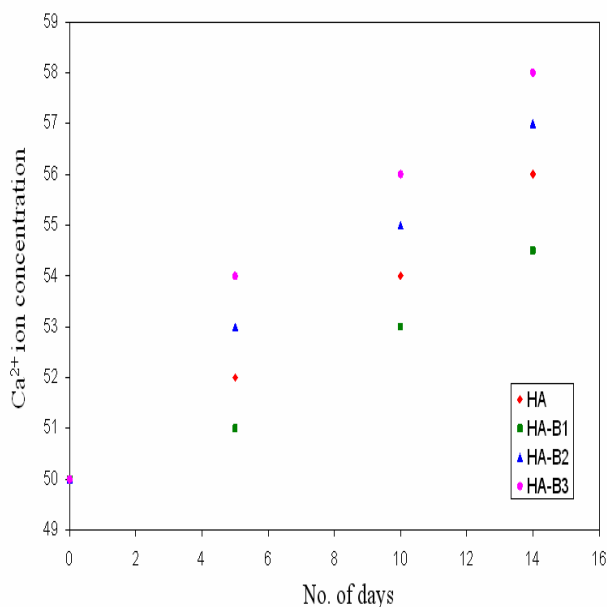


Fig.7. Change in Ca<sup>2+</sup> ion concentration in SBF medium with time

- Solid phase sintering is mainly responsible for bonding in pure HA, whereas liquid phase sintering becomes increasingly prominent with increase in bioglass reinforcement content.
- The density and therefore the hardness as well as the compressive strength of composites increase with increasing bioglass content.
- The mineralization and bioactivity in SBF medium increase with increase in wt % of bioglass in the composite.

#### REFERENCES

- [1] J. C. Knowles, "Development of a glass-reinforced hydroxyapatite with enhanced mechanical properties - the effect of glass composition on mechanical properties and its relationship to phase changes," *J Biomed Mater Res*, 1993, vol. 27, pp. 1591-1598.
- [2] G. Evans, J. Behiri, J. Currey, and W. Bonfield, "Microhardness and Young's modulus in cortical bone exhibiting a wide-range of mineral volume fractions and in a bone analog," *J Mater Sci - Mater Med*, 1990, vol. 1, pp. 38-43.
- [3] H. Aoki, *Science and Medical Applications of Hydroxyapatite*, Tokyo: Takayama Press System Centre, 1991.
- [4] J. C. Knowles, "Development of hydroxyapatite with enhanced mechanical properties - effect of high glass additions on mechanical properties and phase stability of sintered hydroxyapatite," *Br Ceram Trans*, 1994, vol. 93(3), pp. 100-103.
- [5] J. C. Knowles, S. Talal, and J. D. Santos, "Sintering effects in a glass reinforced hydroxyapatite," *Biomaterials*, 1996, vol. 17(14), pp. 1437-1442.
- [6] M. A. Lopes, J. D. Santos, F. J. Monteiro, and J. C. Knowles, "Glass-reinforced hydroxyapatite: a comprehensive study of the effect of glass composition on the crystallography of the composite," *Biomed Mater Res*, 1998, vol. 39(2), pp. 244-251.
- [7] C. Rey, M. Freche, M. Heughebaert, J. C. Heughebaert, J. L. Lacout, and M. Vignoles, *Apatite chemistry in biomaterial preparation*,

- shaping and biological behaviour, In: W. Bonfield, G. W. Hastings, and K. E. Tanner, editors. *Bioceramics*, vol. 4. London: Butterworth Heinemann, 1991.
- [8] R. Z. LeGeros, J. P. LeGeros, An introduction to bioceramics, In: L. L. Hench, and J. Wilson editors, World Scientific: Singapore, 1993.
- [9] J. D. Santos, F. J. Monteiro, and J. C. Knowles, "Liquid-phase sintering of hydroxyapatite by phosphate and silicate glass additions - structure and properties of the composites," *J Mater Sci-Mater Med*, 1995, vol. 6(6), pp. 348-52.
- [10] C. Rey, "Calcium phosphate biomaterials and bone mineral. Difference in composition, structure and properties," *Biomaterials*, 2000, vol. 11, pp. 13-15.
- [11] J. D. Santos, P. L. Silva, J. C. Knowles, S. Talal, and F. J. Monteiro, "Reinforcement of hydroxyapatite by adding P<sub>2</sub>O<sub>5</sub>-CaO glasses with Na<sub>2</sub>O, K<sub>2</sub>O and MgO," *J Mater Sci-Mater Med*, 1996, vol. 7(3), pp. 187-189.
- [12] S. R. Radin, and P. Ducheyne, "Effect of bioactive ceramic composition and structure on in vitro behavior. III. Porous versus dense ceramics," *Biomed Mater Res*, 1994, vol. 28, pp. 1303-1309.
- [13] F. Ye1, X. Lu1, B. Lu1, J. Wang, Y. Shi, L. Zhang, J. Chen, Y. Li, and H. Bu, "A long-term evaluation of osteoinductive HA/β-TCP ceramics in vivo: 4.5 years study in pigs," *J Mater Sci-Mater Med*, 2007, vol. 18, pp. 2173-2178.
- [14] N. Matsushita, H. Terai, T. Okada, K. Nozaki, H. Inoue, S. Miyamoto, and K. Takaoka, "A new bone-inducing biodegradable porous BETA-tricalcium phosphate," *Journal of Biomedical Materials Research - Part A*, 2004, vol. 70, pp. 450-458.
- [15] D. C. Moore, M. W. Chapman, and D. Manske, "The evaluation of a biphasic calcium phosphate ceramic for use in grafting long bone diaphyseal defects," *J Orthop Res*, 1987, vol. 5, pp. 356-365.
- [16] W. Cao, and L. L. Hench, "Bioactive materials," *Ceramics International*, 1996, vol. 22, pp. 493 – 507.
- [17] J. D. Santosa, Lakhani J. Jhab, and F. J. Monteiro, "Surface modifications of glass-reinforced hydroxyapatite composites," *Biomaterials*, 1995, vol. 16, pp. 521-526.
- [18] E. J. Lee, H. E. Kim, and H. W. Kim, "Production of Hydroxyapatite/Bioactive Glass Biomedical Composites by the Hot-Pressing Technique," *Journal of the American Ceramic Society*, 2006, vol. 89, pp. 3593 – 3596.
- [19] D. C. Tancred, A. J. Carr, and B. A. O. McCormack, "The sintering and mechanical behavior of hydroxyapatite with bioglass additions," *J Mater Sci-Mater Med*, 2001, vol. 12, pp. 81-93.
- [20] M. Jarcho, "Calcium Phosphate ceramics as a hard tissue prosthetics," *Biomaterials*, 1981, vol. 12, pp. 157-168.
- [21] Jae-Man Cho, "Formation and characterization of Hydroxyapatite coating layer by electron beam deposition," *Journal of Material Research*, 1999, vol. 14, pp. 145-158.
- [22] C. J. Kirkpatrick, "A critical view of current and proposed methodologies for biocompatibility testing: cytotoxicity in vitro," *Regulatory Affairs*, 1992, vol. 4, pp. 13-32.